Quantum analog of the Kolmogorov-Arnold-Moser theorem in the anisotropic Dicke model and its possible implications in the hybrid Sachdev-Ye-Kitaev models

Yi-Xiang Yu,[1] Jinwu Ye,[2,3] Wu-Ming Liu,[4] and CunLin Zhang[5]
[1]*School of Physics, Beijing Institute of Technology, Beijing, 100081, China*
[2]*Institute for Theoretical Sciences, Westlake University, Hangzhou, 310024 Zhejiang, China*
[3]*Department of Physics and Astronomy, Mississippi State University, P. O. Box 5167, Mississippi State, Mississippi 39762, USA*
[4]*Beijing National Laboratory for Condensed Matter Physics, Institute of Physics, Chinese Academy of Sciences, Beijing 100190, China*
[5]*Key Laboratory of Terahertz Optoelectronics, Ministry of Education and Beijing Advanced Innovation Center for Imaging Technology, Department of Physics, Capital Normal University, Beijing 100048, China*

(Received 30 July 2021; revised 30 November 2021; accepted 28 July 2022; published 19 August 2022)

The classical Kolmogorov-Arnold-Moser (KAM) theorem provides the underlying mechanism for the stability of the solar system under some small chaotic perturbations. Despite many previous efforts, any quantum version of the KAM theorem remains elusive. In this work, we provide a quantum KAM theorem in the context of the anisotropic Dicke model, which is the most important quantum optics model. It describes a single mode of photons coupled to N qubits with both a rotating wave (RW) term and a counter-RW (CRW) term. As the ratio of the CRW over the RW term increases from zero to one, the systems evolves from quantum integrable to quantum chaotic. We establish a quantum KAM theorem to characterize such an evolution quantitatively by both large-N expansion and random matrix theory and find agreement from the two complementary approaches. Connections and differences between the Dicke models and Sachdev-Ye-Kitaev (SYK) or hybrid SYK models are examined. A possible quantum KAM theorem in terms of other quantum chaos criteria such as the quantum Lyapunov exponent is also discussed.

DOI: 10.1103/PhysRevA.106.022213

I. INTRODUCTION

In classical chaos, the Kolmogorov-Arnold-Moser (KAM) theorem [1] describes how an integrable Hamiltonian H_0 responds to a chaotic perturbation ΔH, which makes the total Hamiltonian $H = H_0 + \Delta H$ nonintegrable. It states that if the two conditions are satisfied, i.e., (a) ΔH is sufficiently small and (b) the frequencies ω_i of H_0 are incommensurate, then the system remains quasi-integrable. The classical KAM theorem has played important roles in the stability of the solar system and many other classical chaotic systems. It remains an outstanding problem to find a quantum analog of the KAM theorem for a quantum many-body system. Here, we will try to achieve such a goal in the context of the anisotropic $[J - U(1)/Z_2]$ Dicke model [2,3], given by Eq. (1), which is the most important model in quantum optics.

There are previous works [4–9] studying both quantum phase transitions (QPTs) and quantum chaos in several extreme limits of the $J - U(1)/Z_2$ Dicke model given by Eq. (1). It describes a single mode of photons coupled to N qubits with both a rotating wave (RW) g term and a counter-RW (CRW) g' term at any ratio $\beta = g/g'$. For example, the authors in [4] studied the $J - Z_2$ Dicke model with $\beta = 1$ at the thermodynamic limit $J = \infty$ and also its energy level statistics (ELS) [10,11] at a finite $J = N/2$. In the $J = \infty$ limit, as the atom-photon coupling strength increases above a critical value, it displays a QPT from the normal to the superradiant phase [12,13]. However, the system becomes nonintegrable at any finite J. By studying its ELS by exact diagonalization (ED) at finite sizes $N \geqslant 10$ at a given parity sector, they found that in the normal phase, it is Poissonian, $P_p(s) = e^{-s}$, but in the superradiant phase becomes a Wigner-Dyson (WD) distribution in the Gaussian orthogonal ensemble (GOE) class, $P_w(s) = \frac{\pi}{2} s e^{-\frac{\pi}{4}s^2}$, in the random matrix theory (RMT) classification [10,11]. This fact suggests that the quantum chaotic to integrable transition (CIT) at a finite N may be associated to the QPT at $N = \infty$.

On the other limit, the U(1) Dicke model [5,6] with $\beta = 0$ is always integrable and still undergoes a QPT from the normal to the superradiant phase at $N = \infty$. This fact indicates that a QPT may not be related to a CIT.

In [6,7], we evaluate the whole energy spectrum of the $J - U(1)$ Dicke model (with $J = N/2$) with $\beta = 0$ by a $1/J$ expansion and find nearly perfect agreements with those found from the ED when N is even as small as $N = 2$.

It was well known that quantum dynamics are inherently encoded in any quantum many-body system; one effective way to characterize any possible quantum chaos in such an intrinsic quantum dynamics is through random matrix theory (RMT) [10,11,14]. We first propose a quantum version of the KAM theorem to describe the quantum chaotic to integrable transition (CIT) in terms of the RMT. Then we derive the effective Hamiltonian given by Eq. (1) at any ratio $0 < \beta = g'/g < 1$ by the $1/N$ expansion. By using the effective Hamiltonian, we investigate the analytic scaling form of

the quantum KAM theorem at a finite N near its quantum integrable U(1) limit $\beta = g'/g \ll 1$. By carefully identifying the chaotic source leading to the energy level correlations near the quantum integrable U(1) limit, we show that the quantum KAM theorem given by Eq. (12) holds in the strong-coupling limit $N > g/g_c \gg 1$, so the system remains quasi-integrable. We stress the important roles played by the Berry phase in its establishment. By using the RMT, we evaluate the energy level statistic (ELS) at $N = 10, 20$ at a given parity sector by exact diagonalizations (EDs) at any $0 < \beta < 1$.

The ED data in the RMT fit well with the analytic quantum KAM theorem given by Eq. (12) achieved by the $1/N$ expansion. We explore the intrinsic connections between the QPT characterized by $1/N$ expansions and the CIT characterized by the RMT. Contrasts to the Sachdev-Ye-Kitaev (SYK) and hybrid SYK models [15–19] are made. A possible quantum KAM in terms of the Lyapunov exponent is discussed.

II. THE $1/J$ EXPANSION OF THE $J - U(1)/Z_2$ DICKE MODEL IN THE SUPERRADIANT PHASE AND QPT

In the $J - U(1)/Z_2$ Dicke model [2,3], a single mode of photons couple to N two-level atoms projected in the total angular momentum $J = N/2$ state [6,8],

$$H_J = \omega_a a^\dagger a + \omega_b J_z + \frac{g}{\sqrt{2J}}(a^\dagger J_- + a J_+) + \frac{g'}{\sqrt{2J}}(a^\dagger J_+ + a J_-), \quad (1)$$

where ω_a, ω_b are the energy of the cavity photons and the two atomic levels, respectively; $g = \sqrt{N}\tilde{g}$, $g' = \sqrt{N}\tilde{g}'$ are the collective photon-atom rotating wave (RW) coupling and counter-rotating wave (CRW) term, respectively. If $\beta = g'/g = 0$, Eq. (1) reduces to the U(1) Dicke model [5] with the U(1) symmetry $a \to a e^{i\theta}$, $\sigma^- \to \sigma^- e^{i\theta}$ leading to the conserved quantity $P = a^\dagger a + J_z$, where $J^z = \frac{1}{2}\sum_i \sigma_i^z$. The CRW g' term breaks the U(1) to the Z_2 symmetry $a \to -a$, $\sigma^- \to -\sigma^-$ with the conserved parity operator $\Pi = e^{i\pi(a^\dagger a + J_z)}$. If $\beta = 1$, it becomes the Z_2 Dicke model [4,8]. If $\beta = \infty$, it can be mapped to the static version of the Landau-Zener (LZ) model [20]. In this work, we fix the ratio to be $0 < g'/g = \beta < 1$. The other case with $1 < \beta < \infty$ needs a different treatment and will be discussed in a separate publication [9].

Inside the superradiant phase, it is convenient to write both the photon and atom in the polar coordinates $a = \sqrt{\lambda_a^2 + \delta\rho_a}e^{i\theta_a}$, $b = \sqrt{\lambda_b^2 + \delta\rho_b}e^{i\theta_b}$. We first minimize the ground-state energy at the order J and find the saddle-point values of λ_a and λ_b:

$$\lambda_a = \frac{g + g'}{\omega_a}\sqrt{\frac{j}{2}(1 - \mu^2)}, \quad \lambda_b = \sqrt{j(1 - \mu)}, \quad (2)$$

where $\mu = \omega_a\omega_b/(g + g')^2$. In the superradiant phase, $\mu < 1$, so that $g + g' > g_c^t = \sqrt{\omega_a\omega_b}$. In the normal phase, $g + g' < g_c^t$, one gets back to $\lambda_a = \lambda_b = 0$. At a fixed β, the QPT happens at $g_c = \frac{\sqrt{\omega_a\omega_b}}{1+\beta}$.

Well inside the superradiant phase, $\lambda_a^2 \sim \lambda_b^2 \sim J$, it is convenient to introduce the $\pm$ modes: $\theta_\pm = (\theta_a \pm \theta_b)/2$, $\delta\rho_\pm = \delta\rho_a \pm \delta\rho_b$, $\lambda_\pm^2 = \lambda_a^2 \pm \lambda_b^2$. The Berry phase in the $+$ sector [6] can be defined as

$$\lambda_+^2 = P + \alpha, \quad (3)$$

where $P = 1, 2, \ldots$ is the closest integer to the λ_+^2, so $-1/2 < \alpha < 1/2$.

After shifting $\theta_\pm \to \theta_\pm + \pi/2$, we reach the Hamiltonian to the order of $1/J$,

$$\mathcal{H}[\delta\rho_\pm, \theta_\pm] = \frac{D}{2}(\delta\rho_+ - \alpha)^2 + D_-[\delta\rho_- + \gamma(\delta\rho_+ - \alpha)]^2 + 4\omega_a\lambda_a^2\left[\frac{1}{1+\beta}\sin^2\theta_- + \frac{\beta}{1+\beta}\sin^2\theta_+\right], \quad (4)$$

where $D = \frac{2\omega_a(g+g')^2}{E_H^2 N}$ is the phase diffusion constant in the $+$ sector, $D_- = E_H^2/16\lambda_a^2\omega_a$ with $E_H^2 = (\omega_a + \omega_b)^2 + 4(g + g')^2\lambda_a^2/N$. The $\gamma = \frac{\omega_a^2}{E_H^2}(1 - \frac{(g+g')^4}{\omega_a^4})$ is the coupling between the $+$ and $-$ sectors. Due to the large gap in the θ_- sector when $0 < \beta < 1$, it is justified to drop the Berry phase in the $-$ sector.

It is instructive to rewrite Eq. (4) as

$$\mathcal{H}[\delta\rho_\pm, \theta_\pm] = H_{U(1)} + 4\omega_a\lambda_a^2\frac{\beta}{1+\beta}\sin^2\theta_+, \quad (5)$$

where the $H_{U(1)}$ is the Hamiltonian of the $J - U(1)$ model,

$$H_{U(1)} = \frac{D}{2}(\delta\rho_+ - \alpha)^2 + D_-[\delta\rho_- + \gamma(\delta\rho_+ - \alpha)]^2 + 4\omega_a\lambda_a^2\frac{1}{1+\beta}\sin^2\theta_-, \quad (6)$$

which conserves $\delta\rho_+$. Its eigenenergies and eigenstates are listed in [6] and also reviewed in Appendix A. Equation (5) naturally separates the chaotic perturbation H_c' from those integrable ones. Near the integrable U(1) limit $\beta \ll 1$, the second term H_c' in Eq. (5) can be treated as the small chaotic perturbation $[H_c', H_{U(1)}] \neq 0$; it violates the conservation of $\delta\rho_+$, but still keeps the parity $\Pi = e^{i\pi(P+\delta\rho_+)}$. Although Eq. (6) explicitly contains β dependencies, they still keep the integrability, and so do not change the ELS. This observation will be analyzed further in the following section.

III. A QUANTUM KAM THEOREM: GENERAL STATEMENT

Inspired by the classical KAM theorem, we expect that a quantum analog of the KAM theorem exists near an integrable quantum many-body system whose eigenenergies are in-commensurate. In Eq. (6), it is the frustration due to the Berry phase α which make its eigenenergies incommensurate except at $\alpha = 0, \pm 1/2$, which have zero measures anyway. We state the general form of a quantum KAM theorem from the RMT point of view: *Near the integrable limit of an in-commensurate quantum many-body system, when the energy level repulsion caused by a small chaotic perturbation is less than the average many-body energy spacing of the integrable system, the system remains quasi-integrable, so its ELS remains to be Poissonian.* This is justified because all the energy levels in the integrable side are uncorrelated. Specifically, taking two nearest-neighbor (NN) bulk energy states with the NN

energy level spacing $s_0 = E_2^0 - E_1^0$, one can write the 2×2 quantum chaotic matrix within the two NN energy level subspace as $\Delta_{ij} = \langle i|H_c'|j\rangle$, $i, j = 1, 2$. By a bulk energy level E_B, we mean $\lim_{N\to\infty} \frac{E_B - E_0}{N} \neq 0$, where E_0 is the ground-state energy. Then the perturbed NN energy level spacing is

$$S = \sqrt{s^2 + |\Delta_{12}|^2}, \tag{7}$$

where $s = s_0 + \Delta_{22} - \Delta_{11}$ is the diagonal energy shift due to the chaotic perturbation, and the Δ_{12} is the off-diagonal one. It is important to observe that if setting $\Delta_{12} = 0$ in Eq. (7), then the ELS still stays Poissonian. This is because the diagonal shift does not change the ELS, only the off-diagonal shift does. Indeed, near any integral limit $\mathcal{H}_0$, if one adds a perturbation $\mathcal{H}_1$ which commutes with the integral Hamiltonian $[\mathcal{H}_0, \mathcal{H}_1] = 0$, $\mathcal{H}_1$ is a conserved quantity and the system remains integrable. However, $\mathcal{H}_1$ still induces a diagonal energy shift, but not the off-diagonal one. Obviously, it is the off-diagonal one which introduces the level repulsion between the two NN levels, which, in turn, leads to the change of ELS to WD. So we conclude that when $|\Delta_{12}| < s$ in Eq. (7), the ELS stays Poissonian, and the quantum KAM applies. In the following, instead of giving a rigorous mathematical proof of this quantum KAM theorem, we derive its analytic finite-size scaling form by $1/N$ expansion in Eq. (5) and compare with our ED at various available values of N.

IV. THE QUANTUM KAM THEOREM: THE $1/N$ EXPANSION ON THE DICKE MODEL

Let us take two NN states as $|B1\rangle = |l\rangle_m|m\rangle$ and $|B2\rangle = |l\rangle_{m+2}|m+2\rangle$, where $l \sim N/2$ and $m \sim 1$ with a typical Berry phase $-1/2 < \alpha < 1/2$. Then, $\lim_{N\to\infty} \frac{E_B - E_0}{N} = \hbar\omega_0/2$. One can immediately evaluate the diagonal matrix element $\langle B1|H'|B1\rangle = \langle B2|H'|B2\rangle = 2\omega_a\lambda_a^2\frac{\beta}{1+\beta}$. So the chaotic perturbation does not change the diagonal energy level spacing,

$$s = E_0(l, m+2) - E_0(l, m) = 2D(m - \alpha + 2), \tag{8}$$

which is independent of the Landau level index $l \sim N/2$. This fact simplifies the computation considerably.

One can also compute the splitting (NN energy level repulsion) in terms of the coherent state,

$$\Delta_{12} = \langle B1|H'|B2\rangle = \omega_a\lambda_a^2\frac{\beta}{1+\beta}\,{}_m\langle l|l\rangle_{m+2}, \tag{9}$$

where one can evaluate the matrix element,

$$\begin{aligned} f(l, l) &= {}_m\langle l|l\rangle_{m+2} = \langle l|D(iG)|l\rangle \\ &= e^{-G^2/2} l! \sum_{r=0}^{l} \frac{(-1)^{l-r} G^{2l-2r}}{[(l-r)!]^2 r!}, \end{aligned} \tag{10}$$

where $G = g_{m+2} - g_m = \frac{\sqrt{2}\gamma}{\beta_o}$. One can find $f(0, 0) = e^{-G^2/2}$, $f(1, 1) = e^{-G^2/2}(1 - G^2)$, …. In fact, more straightforwardly, in terms of the wave function of a harmonic oscillator, $f(l, l) = \int d\theta_- |\psi_l(\theta_-)|^2 e^{i2\gamma\theta_-}$, $l = 1, 2, 3, \ldots$, one reaches the same results as Eq. (10).

One can write the general expressions of the three quantities λ_a^2 in Eq. (2), the diffusion constant D in Eq. (4), and $G^2/2$ in Eq. (10) in terms of $g/g_c > 1$ inside the superradiant phase. They simplify dramatically in the strong-coupling limit $N > g/g_c \gg 1$,

$$\begin{aligned} \lambda_a^2 &= \left(\frac{g}{g_c}\right)^2 N, \\ D &= 2\omega\left(\frac{g}{g_c}\right)^{-2}\frac{1}{N} \sim 2\omega/\lambda_a^2, \\ G^2/2 &= \frac{\sqrt{1+\beta}}{2}\frac{1}{N}. \end{aligned} \tag{11}$$

In the large-N limit, the polynomial in $f(l = N/2, l = N/2)$ multiplying the exponential $e^{-G^2/2}$ becomes $(1 - \frac{1}{2} + \frac{1}{36} - \frac{1}{8\times 36} + \cdots)$. So we conclude that $f(N/2, N/2) \sim e^{-G^2/2}/2$ as $N \to \infty$.

Applying the general criterion to the two typical bulks states in Eq. (8) and Eq. (9) leads to a scaling form of the quantum KAM theorem,

$$\beta_{c1} \sim N^{-2} e^{1/2N} (g/g_c)^{-4}, \tag{12}$$

which approaches zero in both the thermodynamic limit $N \to \infty$ and the strong-coupling limit $N > g/g_c \gg 1$.

One may also propose the quantum KAM theorem from a dual point of view, namely, from the chaotic Z_2 limit at $\beta = 1$ inside the super-radiant phase in Figs. 1 and 2, namely, investigate how the chaotic behaviors change to integrable as the perturbation $1 - \beta$ increases. There is no change of the symmetry as $1 - \beta$ turns on; the stability of quantum chaos is much more robust than the KAM in the integrable side. If we define β_{c2} as the dual form of the KAM theorem in Fig. 2, then β_{c2} remains finite as $N \to \infty$. Inside the superradiant phase $g/g_c \geqslant 1$, when $\beta_{c2} < \beta < 1$, it remains chaotic. When $\beta_{c1} < \beta < \beta_{c2}$, the ELS is in a crossover regime and satisfies neither GOE nor Poissonian. When $0 < \beta < \beta_{c1}$, it reaches the quantum KAM regime.

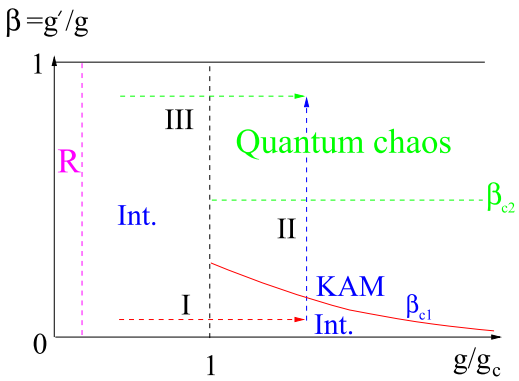

FIG. 1. QPT vs CIT in the large-N limit. The U(1) limit $\beta = 0$ is integrable, only QPT. In the Z_2 limit $\beta = 1$, the QPT is accompanied by the CIT. The quantum KAM scaling $\beta_{c1} \sim N^{-2}$ given by Eq. (12) achieved by $1/N$ expansion matches qualitatively with that extracted from the ED in RMT in Fig. 2. β_{c2} sets the quantum chaotic regime (or dual KAM), which remains finite as $N \to \infty$. R one the left means the regular regime [21]. Path I: QPT tuned by the coupling g/g_c, with no CIT. Path II: CIT tuned by β, with no QPT. Path III: The QPT is accompanied by the CIT.

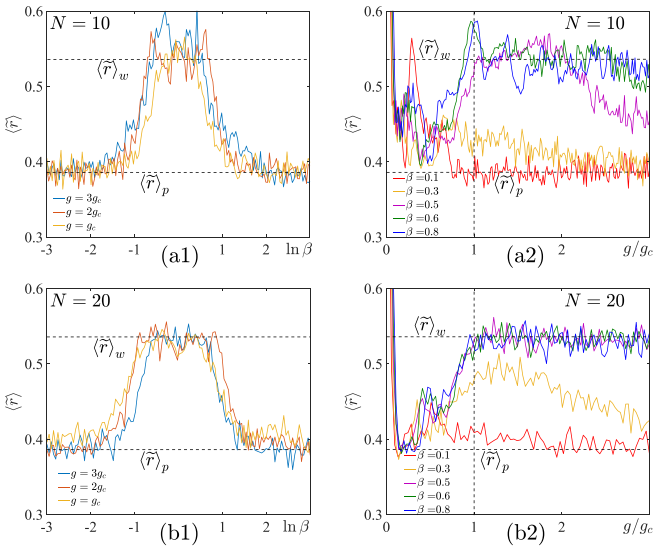

FIG. 2. The mean values of the ratio $\widetilde{r}$ evaluated by ED at (a) $N = 10$ and (b) $N = 20$ at the resonant case $\omega_a = \omega_b$. The off-resonant case can also be similarly discussed. The analytical mean values of $\widetilde{r}$ of Poisson $\langle\widetilde{r}\rangle_p$ and GOE $\langle\widetilde{r}\rangle_w$ are marked as references. (a1) The CIT at a fixed $g/g_c \geqslant 1$ at three values $g/g_c = 3, 2, 1$ and tuning $\ln\beta$. See path II in Fig. 1. One can identify the KAM regime as $\ln\beta_{c1} \sim \pm 1.2$, which leads to $\beta_{c1} \sim 0.3$ near $g/g_c > 1$. One may also identify the stability regime of the quantum chaos as $\ln\beta_{c2} \sim \pm 0.5$, which leads to $\beta_{c2} \sim 0.6$. When $\beta_{c1} < \beta < \beta_{c2}$, there is no well-defined ELS. (a2) At a fixed β vs g/g_c at five different values, $\beta = 0.1, 0.3, 0.5, 0.6, 0.8$. See paths III and I in Fig. 1. One may also identify $\beta_{c1} \sim 0.3$, $\beta_{c2} \sim 0.6$. When $\beta_{c2} < \beta < 1$ (path III in Fig. 1), there is an accompanying CIT near the QPT at $g/g_c = 1$, but when $0 < \beta < \beta_{c1}$ (path I in Fig. 1), there is no such accompanying transition. In both cases, when $g/g_c < 0.15$, $\widetilde{r}$ shoots up to 1, and the system just tends to be regular instead of random [21]. (b) The ED data at $N = 20$ has less noise due to the larger finite size. Compared to $N = 10$ in (a), one can see that in (b1), when $g/g_c \geqslant 1$, the quantum chaos regime expands and the integrable regime shrinks. One can identify $\beta_{c2} \sim 0.5$. (b2) At the same set of β as (a2). The line with the same color (β) is elevated towards the chaotic side, indicating β_{c1} drops as N increases. One can see $\beta_{c1} \sim 0.1$ near $g/g_c > 1$. Our ED results also show that β_{c1} decreases at a fixed $N = 20$ and much larger $g/g_c \sim 10 - 20 \gg 1$, also in qualitative agreement with Eq. (12).

V. THE ENERGY LEVEL STATISTICS IN RMT AND THE CIT

Now we look at the RMT classification of Eq. (1). The time-reversal symmetry is simply the complex conjugate operator $\mathcal{T} = K$ which acts as $KaK^{-1} = a$, $Ka^{\dagger}K^{-1} = a^{\dagger}$, $KiK^{-1} = -i$. Obviously, $KJ_aK^{-1} = J_a$, $a = \pm, z$. It keeps the commutation relations $[a, a^{\dagger}] = 1$, $[J_z, J_{\pm}] = \pm J_{\pm}$. So the many-body Hamiltonian given by Eq. (1) has the time-reversal symmetry, also $K^2 = 1$, so it satisfies GOE.

As shown in [14–18] and reviewed in Appendix B, the most effective way to characterize an ELS is to study the distribution of the ratio of two NN energy level spacings $\langle\widetilde{r}\rangle$. We plot $\langle\widetilde{r}\rangle$ vs $\ln\beta$ at a fixed $g/g_c = 3, 2, 1$ and $\langle\widetilde{r}\rangle$ vs g/g_c at a fixed $\beta = 0.1, \ldots, 0.8$ in Fig. 2(a) and Fig. 2(b), respectively, for two different sizes $N = 10, 20$. The data $\beta_{c1} \sim 0.3, 0.1$ at the two different sizes $N = 10, 20$ qualitatively match the scaling in Eq. (12). A small discrepancy may be attributed to the cutoff introduced in the ED (see Appendix C).

VI. CONTRAST ANISOTROPIC DICKE MODELS WITH HYBRID SYK MODELS

So far we have focused on the $U(1)/Z_2$ anisotropic Dicke model, which is the most important model in quantum optics. The quantum chaos in the Dicke model is investigated here by both $1/N$ expansion and RMT. Similar approaches have also been used to explore the quantum chaos in the Sachdev-Ye-Kitaev (SYK) model, which may be dual to a quantum black hole [15–19,22–24]. It is constructive to contrast the (anisotropic) Dicke model to the (hybrid) SYK models. (a) Both have an infinite-range interaction, so are effectively $(0 + 1)$-dimensional systems. (b) Both show quantum chaos and quantum information scramblings which can be studied by $1/N$ expansion and random matrix theory (RMT), respectively. But the mechanism leading to the quantum chaos is very different. The former is due to both interactions and disorders. The latter is due to the atom-photon interactions. (c) The former is an interacting fermionic model with quenched disorders, while the latter is a clean interacting bosonic one consisting of N qubits interacting with photons. So when performing the ED in RMT, the Hilbert space in the former is automatically finite, $\sim 2^N$, while the latter is infinite, so a finite cutoff needs to be introduced (see Appendix C). (d) The ground state of SYK is a conformably invariant gapless quantum spin liquid which leads to the maximal Lyapunov exponent $\lambda_L = 2\pi/\beta$ by $1/N$ expansion when $1 < \beta J < N$. In the superradiant phase in the Dicke model, there is a symmetry breaking in the $N \to \infty$ limit, but the symmetry breaking is restored at a finite N by the quantum tunneling process [8]. So it has a finite gap $\sim \omega$ at a given parity sector in the strong-coupling $g/g_c \gg 1$ limit, the quantum Lyapunov exponent $\lambda_L = 0$ in the low-temperature range $1 < \beta\omega < N$. However, we expect $\lambda_L = g[1 - (1 - \beta) + \cdots]$ when $T \gg \omega$ and reach the maximum at the Z_2 limit $\beta = 1$ and vanish when $\beta < \beta_{c1}$. (e) Various hybrid SYK models [18] also hold various CITs from the quantum integrable side of the $q = 2$ SYK to the quantum chaotic side of the $q = 4$ SYK tuned by the ratio of the couplings of the two sides. We expect that the general statement on a KAM theorem in Sec. III still applies to the hybrid SYK models. Some preliminary results on the scaling forms of a quantum KAM in the hybrid SYK contexts are presented in [18]. However, due to the quenched disorders, constructing a rigorous quantum KAM to characterize the CIT in the hybrid SYK models may be more challenging, but important, to pursue.

VII. CONCLUSIONS

In this work, we take a 2×2 matrix spanned by two typical NN bulk energy levels to find the quantum KAM scaling given by Eq. (12). This is justified because all the energy levels in the integrable side are uncorrelated. In principle, one may also take all the bulk energy levels. However, as shown in [10] and reviewed in Appendix B, by considering a $L \times L = 2 \times 2$ matrix, Wigner derived a simple approximate expression for

the distribution function $P(s)$ of the NN spacing for GOE, Gaussian unitary ensemble (GUE), and Gaussian symplectic ensemble (GSE), respectively. Although this so-called Wigner surmise was achieved only for 2×2 matrices, it is in very good agreement with the exact large-L expressions. We expect a similar thing happens here: the exact $L \to \infty$ calculation will only slightly modify the prefactor in Eq. (12). The qualitative agreement between our analytical KAM scaling given by Eq. (12) with the ED data in the RMT supports this claim. It is important to extend the concepts and methods developed here for interacting bosonic systems to interacting fermionic systems with quenched disorders such as the hybrid SYK models.

It remains outstanding to construct a quantum KAM theorem through the Lyapunov exponent or any other criterion characterizing the quantum chaos in the context of both Dicke and SYK models. It is also interesting to establish some quantum-classical correspondence between the classical KAM and the quantum KAM in the context of driven nonequilibrium Dicke [25] or driven nonequilibrium SYK [26] models.

ACKNOWLEDGMENTS

J.Y. thanks Fadi Sun for inspiring discussions on RMT and the collaboration on the possible quantum analog of the KAM theorem in the various hybrid SYK models [18]. This work was supported by NSF of China (grants No. 12104042, and No. 61835013) and China Postdoctoral Science Foundation (grant No. 2018M640190). C.L.Z.'s work has been supported by the National Keystone Basic Research Program under Grants No. 2007CB310408 and No. 2006CB302901.

APPENDIX A: THE EIGENENERGY AND EIGENFUNCTIONS IN THE $1/N$ EXPANSION

Let us start with Eq. (5). Obviously, for $[H_{U(1)}, \delta\rho_+] = 0$, the $\delta\rho_+$ is a conserved quantity, so one can find the simultaneous eigenstates of $H_{U(1)}$ and $\delta\rho_+$, which will be achieved in the following.

As explained in Sec. II, the θ_- is very massive; after pinning θ_- around $\theta_- \sim 0$, one can approximate $\sin^2\theta_- \sim \theta_-^2$, and therefore one may ignore the Berry phase in the θ_- sector. Then the above equation can be simplified to

$$H_{U(1)} = \frac{D}{2}(\delta\rho_+ - \alpha)^2 + D_-[\delta\rho_- + \gamma(\delta\rho_+ - \alpha)]^2 + 2\omega_a\lambda_a^2\frac{2}{1+\beta}(\theta_-)^2, \tag{A1}$$

whose wave functions can be written as $|m\rangle|l\rangle_m$, where

$$\langle\theta_+|m\rangle = \frac{1}{\sqrt{2\pi}}e^{im\theta_+}, \langle\theta_-|l\rangle_m = e^{i\gamma(m-\alpha)\theta_-}\psi_l(\theta_-), \tag{A2}$$

where the $\psi_l(\theta_-)$ is just the lth wave function of a harmonic oscillator. So the total wave function $\psi_{l,m}(\theta_+, \theta_-) = \langle\theta_+, \theta_-|m\rangle|l\rangle_m$ is

$$\psi_{l,m}(\theta_+, \theta_-) = \frac{1}{\sqrt{2\pi}}e^{i(m\theta_+ + \gamma(m-\alpha)\theta_-)}\psi_l(\theta_-), \tag{A3}$$

where the wave function is only periodic in $0 < \theta_+ < 2\pi$, and the $-\infty < \theta_- < \infty$ is treated as a continuous variable. The corresponding eigenenergy is

$$E_0(l, m) = (l + 1/2)\hbar\omega_o + \frac{D}{2}(m - \alpha)^2, \tag{A4}$$

where the $\omega_o = E_H/\sqrt{1+\beta}$ and where $E_H^2 = (\omega_a + \omega_b)^2 + 4(g + g')^2\lambda_a^2/N$ is defined below in Eq. (4).

It is important to observe that Eq. (A1) still contains β dependence. Only setting $\beta = 0$ in Eq. (A1) recovers the $1/N$ expansion of the original Eq. (1). As stressed below Eq. (6), despite Eq. (A1) explicitly contains β dependencies, they still keep the integrability, so do not change the ELS. So it is a good starting point to look at the effects of a chaotic perturbation.

Note that the Landau level index $l = 0, 1, \ldots, N$ ($N + 1$ Landau levels) denotes the high-energy Higgs type of excitation, while the magnetic number $m = -P + l, -P + l + 1, \ldots$ (no upper bounds) denotes the low-energy Goldstone types of excitations. The total parity is $\Pi = (-1)^{P+m}$ at the sector P, where $P \geqslant l + 1$ has no upper bound either. At a given Landau level l and a given sector P, there are $|m| = P - l \geqslant 1$ crossings at the Berry phase $\alpha = 0$ in Eq. (A4). The $m = 0$ is always the ground-state energy at a given l and a given $P \geqslant l + 1$.

In the large-($J = N/2$) limit, $\omega_o \gg D \sim 1/j$, so the first term can be considered as the inter-Landau levels, while the second term can be considered as the intra-Landau levels.

It is instructive to look at the harmonic oscillator in the $-$ sector from an algebraic point of view. Define $\beta_o = \sqrt{\frac{\mu\omega_o}{\hbar}}$, where $\mu = \frac{1}{2D_-}$ is the mass of the harmonic oscillator. The annihilation operator $a_- = \frac{1}{\sqrt{2}}(\beta_o\theta_- + i\frac{\delta\rho_-}{\beta_o\hbar})$. Then, after making a momentum shift $\delta\rho_- \to \delta\rho_- - \gamma(\delta\rho_+ - \alpha)$, the annihilation operator $a_- \to a_{-,m} = a_- + i\frac{\gamma(m-\alpha)}{\sqrt{2}\beta_o}$, and the harmonic oscillator's Hamiltonian is $H_- = (a_{-,m}^\dagger a_{-,m} + 1/2)\hbar\omega_o$. Its eigenstate $a_{-,m}^\dagger a_{-,m}|l\rangle_m = l|l\rangle_m$ is

$$|l\rangle_m = D^\dagger(ig_m)|l\rangle = D(-ig_m)|l\rangle, \tag{A5}$$

where $g_m = \frac{\gamma(m-\alpha)}{\sqrt{2}\beta_o}$ and $|l\rangle$ is just the lth harmonic oscillator eigenstate. In particular, the ground state $|0\rangle_m = D(-ig_m)|0\rangle$ is a coherent state.

One can show that $D(-ig_m) = e^{i\gamma(m-\alpha)\theta_-}$, then $|l\rangle_m = e^{i\gamma(m-\alpha)\theta_-}|l\rangle$. So $\langle\theta_-|l\rangle_m = e^{i\gamma(m-\alpha)\theta_-}\langle\theta_-|l\rangle = e^{i\gamma(m-\alpha)\theta_-}\psi_l(\theta_-)$, and we recover Eq. (A2) from the coherent state.

APPENDIX B: A BRIEF REVIEW OF RANDOM MATRIX THEORY AND THE ENERGY LEVEL STATISTIC (ELS) OF NEAREST NEIGHBOR (NN) ENERGY LEVEL SPACINGS

For the three Wigner-Dyson classes, i.e., A(GUE), AI(GOE), and AII(GSE), no mirror symmetry exists in the energy levels. Let $\{E_n\}$ be an ordered set of energy levels; then the joint probability distribution for all the eigenvalues can be described by

$$P(\{E_i\}) \propto \prod_{i<j}|E_i - E_j|^\beta \prod_n e^{-E_n^2}, \tag{B1}$$

where β is the Wigner-Dyson index characterizing the strength of level repulsion. For class A(GUE), AI(GOE), and AII(GSE), $\beta = 2, 1, 4$, respectively.

One can denote $s_n = E_{n+1} - E_n$ as the NN spacings. By considering a 2×2 matrix in Eq. (B1), Wigner [10] derived a simple approximate expression for the distribution function $P(s)$ of the NN spacing,

$$P_{w,\beta}(s) = a_\beta s^\beta e^{-b_\beta s^2}, \tag{B2}$$

where $\beta = 1, 2, 4$ is the Dyson index for GOE, GUE, and GSE, respectively. Although this so-called Wigner surmise was achieved only for 2×2 matrices, it is in very good agreement with the exact large-N expressions.

It is also known that independent random energy levels would yield a Poisson distribution

$$P_p(s) = e^{-s}. \tag{B3}$$

However, in order to compare different results from different systems, the energy levels will need an unfolding procedure, which is not convenient when large enough statistics is not available. To get rid of the dependence on the local density of states, it is convenient to look at the distribution of the ratio of two adjacent energy level spacings [14–18], $r_n = s_n/s_{n+1}$, which distributes around 1. This quantity has the advantage that it requires no unfolding since the ratios of consecutive level spacings are independent of the local density of states.

By considering a 3×3 matrix system, the authors in [14] obtained the Wigner-like surmises of the ratio of consecutive level spacings distribution,

$$P_p(r) = \frac{1}{(1+r)^2}, \quad P_w(r) = \frac{1}{Z_\beta} \frac{(r+r^2)^\beta}{(1+r+r^2)^{1+3\beta/2}}, \tag{B4}$$

where $\beta = 1, 2, 4$ and $Z_\beta = 8/27, 4\pi/81\sqrt{3}, 4\pi/729\sqrt{3}$ for GOE, GUE, and GSE, respectively. The distribution $P_W(r)$ has the same level repulsion at small r as $P_W(s)$, namely, $P_W(r) \sim r^\beta$. However, the large-r asymptotic behavior $P_W(r) \sim r^{-(2+\beta)}$ is dramatically different than the fast exponential decay of $P_W(s)$.

One may also compute the distribution of the logarithmic ratio [14,15] $P(\ln r) = P(r)r$. Because $P(\ln r)dr$ is symmetric under $r \leftrightarrow 1/r$, one may confine $0 < r < 1$ and double the probability density $P(\tilde{r}) = 2P(r)$. Therefore, the above two distributions have two different sets of expected values of $\tilde{r} = \min\{r, 1/r\}$:

$$\langle \tilde{r} \rangle_p = \int_0^1 2rP_p(r)dr = 2\ln 2 - 1 \approx 0.38629,$$
$$\langle \tilde{r} \rangle_w = \int_0^1 2rP_{w,\beta=1,2,4}(r)dr, \tag{B5}$$

which is $4 - 2\sqrt{3} \approx 0.53590$, $2\sqrt{3}/\pi - 1/2 \approx 0.60266$, and $32\sqrt{3}/(15\pi) - 1/2 \approx 0.67617$ for GOE, GUE, and GSE, respectively. These Wigner-like surmises given by Eqs. (B4) and (B5) were also shown to be very accurate when compared to the numerics and exact calculations in the exact large-N expressions.

In the main text, the CIT is from the GOE to the Poisson, so only the two values $\langle \tilde{r} \rangle_p \approx 0.38629$ and $\langle \tilde{r} \rangle_{GOE} \approx 0.53590$ are used and plotted in Fig. 2.

APPENDIX C: THE HIGH-ENERGY CUTOFF IN THE EXACT DIAGONALIZATIONS (ED)

We do the ED in Fig. 2 on the $J - U(1)/Z_2$ Dicke model given by Eq. (1) in the Fock basis where the complete basis is $|n\rangle|j, m\rangle$, $n = 0, 1, 2, \ldots, \infty$, $j = N/2$, $m = -j, \ldots, j$, where the n is the number of photons and the $|j, m\rangle$ are the Dicke states. In performing the ED, following Ref. [5], one has to use a truncated basis $n = 0, 1, \ldots, n_c$ in the photon sector where the $n_c \sim 500$–$2000 \gg N$ is the maximum photon number in the artificially truncated Hilbert space. The total number of states is $n_c \times (2j+1) = n_c \times (N+1)$. This is also the size of the RMT, $L = n_c \times (N+1)$. The average many-body energy level spacing at a given parity sector is $\frac{n_c\omega_a}{2n_c\times(N+1)} \sim \frac{\omega_a}{2(N+1)}$. This qualitative estimate is consistent with Eq. (8) achieved by the systematic $1/N$ expansion. As long as the energy levels in Fig. 2 are well below $n_c\omega_a$, the energy levels should be very close to the exact results without the truncation (namely, sending $n_c \to \infty$). However, the ED may no longer be precise when g gets too close to the upper cutoff.

[1] A. N. Kolmogorov, On the conservation of conditionally periodic motions under small perturbation of the Hamiltonian, Dokl. Akad. Nauk SSR **98**, 527 (1954); V. I. Arnold, Proof of a theorem of A. N. Kolmogorov on the preservation of conditionally periodic motions under a small perturbation of the Hamiltonian, Usp. Mat. Nauk. **18**, 13 (1963); J. Moser, On invariant curves of area-preserving mappings of an annulus, Nachr. Akad. Wiss. Göttingen, **II**, 1 (1962).

[2] D. F. Walls and G. J. Milburn, *Quantum Optics* (Springer-Verlag, Berlin, 1994).

[3] M. O. Scully and M. S. Zubairy, *Quantum Optics* (Cambridge University Press, Cambridge, 1997).

[4] C. Emary and T. Brandes, Quantum Chaos Triggered by Precursors of a Quantum Phase Transition: The Dicke Model, Phys. Rev. Lett. **90**, 044101 (2003); Chaos and the quantum phase transition in the Dicke model, Phys. Rev. E **67**, 066203 (2003). It was shown that only when $N \geqslant 6$ does it make sense to talk about the ELS. For example, for the $N = 1$ case, which is the Rabi model, it makes no sense to study its ELS.

[5] K. Hepp and E. H. Lieb, Ann. Phys. **76**, 360 (1973); Y. K. Wang and F. T. Hioe, Phys. Rev. A **7**, 831 (1973); V. N. Popov and S. A. Fedotov, Sov. Phys. JETP **67**, 535 (1988); V. Bužek and V. S. Yarunin, *Collective Effects in Quantum Statistics of Radiation and Matter* (Kluwer Academic, Dordrecht, 1988); V. Buzek, M. Orszag, and M. Rosko, Phys. Rev. Lett. **94**, 163601 (2005); J. Ye and CunLin Zhang, Super-radiance, photon condensation and its phase diffusion, Phys. Rev. A **84**, 023840 (2011).

[6] Yu Yi-Xiang, J. Ye, and W. M. Liu, Goldstone and Higgs modes of photons inside a cavity, Sci. Rep. **3**, 3476 (2013).

[7] Yu Yi-Xiang, J. Ye, W. M. Liu, and CunLin Zhang, Comments on "Controlling discrete and continuous symmetries in superradiant phase transitions with circuit QED systems", arXiv:1506.06382.

[8] Yu Yi-Xiang, J. Ye, and CunLin Zhang, Parity oscillations and photon correlation functions in the $Z_2/U(1)$ Dicke model at a finite number of atoms or qubits, Phys. Rev. A **94**, 023830 (2016).

[9] There is also a recent numerical study on the quantum chaos in the $J-U(1)/Z_2$ Dicke model: W. Buijsman, V. Gritsev, and R. Sprik, Nonergodicity in the Anisotropic Dicke Model, Phys. Rev. Lett. **118**, 080601 (2017). This purely numerical paper did not (1) perform any $1/N$ expansion at a finite N, (2) touch the KAM theorem at a finite N, or (3) explore the intrinsic relations between the CIT at a finite N and the normal to superradiant QPT at $N=\infty$. This paper also made a technical mistake to identify the $0<\beta<1$ case with the $1<\beta<\infty$ case. As argued below Eq. (1), the $g=0$ case in Eq. (1) can be mapped to the static version of the Landau-Zener (LZ) model [20]. In this work, we fix the ratio to be $0<g'/g=\beta<1$. The other case with $1<\beta<\infty$ needs a completely different treatment and will be discussed in a separate publication.

[10] E. P. Wigner, On the statistical distribution of the widths and spacings of nuclear resonance levels, Proc. Cambridge Philos. Soc. **47**, 790 (1951).

[11] F. Dyson, Statistical theory of the Energy Levels of Complex Systems. I, J. Math. Phys. **3**, 140 (1962).

[12] A. Auerbach, *Interacting Electrons and Quantum Magnetism* (Springer Science & Business Media, New York, 1994).

[13] S. Sachdev, *Quantum Phase Transitions*, 2nd ed. (Cambridge University Press, Cambridge, 2011).

[14] Y. Y. Atas *et al.*, Distribution of the Ratio of Consecutive Level Spacings in Random Matrix Ensembles, Phys. Rev. Lett. **110**, 084101 (2013).

[15] Y.-Z. You, A. W. W. Ludwig, and C. Xu, Sachdev-ye-kitaev model and thermalization on the boundary of many-body localized fermionic symmetry protected topological states, Phys. Rev. B **95**, 115150 (2017).

[16] J. S. Cotler, G. Gur-Ari, M. Hanada, J. Polchinski, P. Saad, S. H. Shenker, D. Stanford, A. Streicher, and M. Tezuka, Black holes and random matrices, J. High Energ. Phys. 05 (2017) 118.

[17] F. Sun and J. Ye, Periodic Table of SYK and Supersymmetric SYK, Phys. Rev. Lett. **124**, 244101 (2020).

[18] F. Sun, Yu Yi-Xiang, J. Ye and WuMing Liu, A new universal ratio in Random Matrix Theory and chaotic to integrable transition in Type-I and Type-II hybrid Sachdev-Ye-Kitaev models, Phys. Rev. B **104**, 235133 (2021).

[19] R. Feng, G. Tian, and D. Wei, Spectrum of SYK model, Peking Math. J. **2**, 41 (2019); Spectrum of SYK model II: Central limit theorem, Random Matrices Theory Appl. **10**, 2150037 (2021); Spectrum of SYK model III: Large deviations and concentration of measures, **9**, 2050001 (2020).

[20] A. Altland, V. Gurarie, T. Kriecherbauer, and A. Polkovnikov, Nonadiabaticity and large fluctuations in a many-particle Landau-Zener problem, Phys. Rev. A **79**, 042703 (2009).

[21] Note that in Figs. 2(a2) and 2(b2), there is always a regular regime when $g/g_c<0.15$. This is because in Eq. (1), as $g\to 0$, at a fixed $\beta=g'/g$, $g'\to 0$, only the first two terms survive $H_0=\omega_a[a^\dagger a+J_z]$, which is clearly regular.

[22] S. Sachdev and J. Ye, Gapless Spin Liquid Ground State in a Random Quantum Heisenberg Magnet, Phys. Rev. Lett. **70**, 3339 (1993).

[23] A. Y. Kitaev, Talks at KITP, University of California, Santa Barbara, Entanglement in Strongly-Correlated Quantum Matter (2015).

[24] J. Maldacena and D. Stanford, Remarks on the Sachdev-Ye-Kitaev model, Phys. Rev. D **94**, 106002 (2016).

[25] K. Baumann, R. Mottl, F. Brennecke, and T. Esslinger, Exploring Symmetry Breaking at the Dicke Quantum Phase Transition Phase Transition, Phys. Rev. Lett. **107**, 140402 (2011). Despite the claim made by these authors, the Dicke model realized here is not the equilibrium Dicke one studied here. It may be so in the rotating frame with the pumping laser, but it is a driven nonequilibrium Dicke model in the laboratory frame.

[26] C. Kuhlenkamp and M. Knap, Periodically Driven Sachdev-Ye-Kitaev Models, Phys. Rev. Lett. **124**, 106401 (2020).